

Applying a Priori Information to Computed Laminography

Christian SCHORR¹, Laura DÖRR¹, Michael MAISL¹

¹ Fraunhofer-Institut für Zerstörungsfreie Prüfverfahren IZFP, Campus E3.1, 66123 Saarbrücken,
Phone: +49 681 9302 3935; Fax : +49 681 9302 5901; e-mail: christian.schorr@izfp.fraunhofer.de,
laura.doerr@izfp.fraunhofer.de, michael.maisl@izfp.fraunhofer.de

Abstract.

Reconstructed 3D volumes from computed laminography data suffer from blurring artefacts due to the laminographic geometry. Such losses in quality can be tackled by the use of a priori information about the test object which can be integrated into the iterative reconstruction process. However, this requires the position of the a priori model to be fitted exactly to the measured data. A (semi-)automatic 2D-3D registration algorithm which only requires a minimal additional user input and is based on a mathematical optimization problem is presented. Using measurement data obtained by simulating x-ray projections of the laminographic scanner CLARA the algorithm is legitimated and the results are evaluated.

Keywords: Computed tomography, computed laminography, CLARA, a priori information, 2D-3D registration

1. Introduction

Over the last few decades, computed tomography (CT) has become a well-established and widely used method of nondestructive testing. Still there are some test cases in which this powerful technique for investigating the test object's inner structure is not applicable. For instance, if a planar object, i.e. a potentially very large but extremely flat object, is to be measured using CT two major problems arise. The first of which is caused by the extreme differences in the object's diameters in longitudinal and transversal direction. As CT relies on a full rotation of 360° the object needs to be penetrated by X-rays from each direction. In order for the X-rays not to be fully attenuated when passing through the object in longitudinal direction, their energy has to be sufficiently high which in turn leads to very weak contrast in transversal directions and may result in unusable measurements. The second problem is encountered when aiming for a high magnification ratio. The latter is increased by reducing the distance between object and X-ray source. Especially for fine-structured planar objects the feasible magnification factor may require the object to be so close to the detector that a full object rotation is no longer possible without causing a collision of object and X-ray tube. Both these problems are solved by computed laminography (CL).

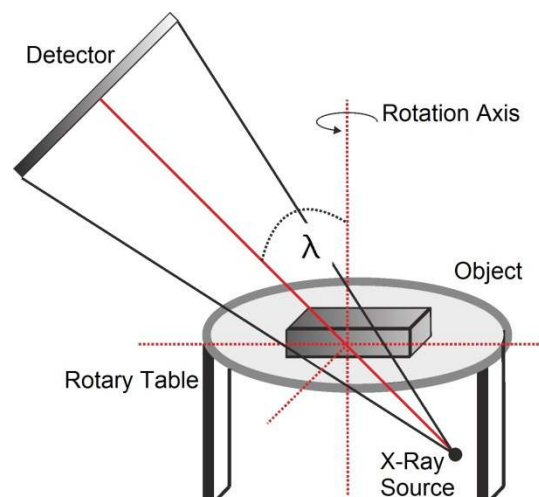


Figure 1. CLARA geometrical composition.

Contrary to traditional CT, for this X-ray technique, neither does the axis between source and detector need to be perpendicular to the rotation axis, nor does the rotation performed necessarily need to measure 360°. There are numerous different CL geometries, some relying on linear or planar translations of the components (classical CL), others representing a tilted version of the traditional CT geometry using a 360° rotation (CLARA) [1]. Using this trajectory, the object can be placed arbitrarily close to the X-ray tube without risking a collision with the latter, thereby enabling an appropriate magnification factor.

2. A priori Information

While allowing for a high-resolution measurement of planar objects, computed laminography also comes with some drawbacks which have to be addressed. Most important, the 3D reconstructions computable from CL data exhibit a lower depth resolution than CT reconstructions. In case of the CLARA geometry, this is due to the constrained information obtainable from the diagonal ray directions. As the (planar) object is always irradiated from the same side, the information gained is not as complete as in a CT (where all rays lie in a horizontal plane). Therefore, CL reconstructions typically show artefacts and blurring orthogonal to the so-called focus plane. This plane, which is always normal to the rotation axis, is the only one fully reconstructable by the measured data. Furthermore, CL data cannot be reconstructed using standard CT algorithms of filtered back projection type like the Feldkamp algorithm. Instead, iterative methods like SART (simultaneous algebraic reconstruction technique) [2] have to be applied.

The SART algorithm models the measurement process as a system of linear equations and tries to solve it iteratively. Let the 3D volume consisting of n voxels with indices $j = 1, \dots, n$ be described by $f \in \mathbb{R}^n$, the measured rays be given by $p_i, i = 1, \dots, m$ and ω_{ij} correspond to the fraction of the i -th ray p_i passing through pixel j . Then, each SART iteration reads

$$f_j^{(k+1)} = f_j^{(k)} + \lambda \cdot \frac{\sum_{p_i \in P_\alpha} \left(\frac{p_i - \sum_{l=1}^n \omega_{il} f_l^{(k)}}{\sum_{l=1}^n \omega_{il}} \right)}{\sum_{p_i \in P_\alpha} \omega_{ij}} \quad (1)$$

Where $\lambda \in \mathbb{R}$ is a relaxation factor and P_α the set of rays belonging to projection $\alpha, \alpha \in \{\alpha_1, \dots, \alpha_p\}$. A priori information can easily be integrated into this reconstruction process if it is given as a second, binary voxel volume g of the same dimensions as the volume to be reconstructed, i.e. $g \in \{0,1\}^n$ with g_j giving the probability of voxel j containing any material. In this case, the a priori SART iteration step is given by

$$f_j^{(k+1)} = f_j^{(k)} + g_j \cdot \lambda \cdot \frac{\sum_{p_i \in P_\alpha} \left(\frac{p_i - \sum_{l=1}^n \omega_{il} f_l^{(k)}}{\sum_{l=1}^n \omega_{il}} \right)}{\sum_{p_i \in P_\alpha} \omega_{ij}} \quad (2)$$

This straight-forward integration of a priori information not only increases the convergence speed of the reconstruction process but at the same time offers the possibility of reducing the blurring artefacts characteristic for computed laminography reconstructions as well as increasing contrast. As a result, defects become more easily detectable [3,4]. As a priori information given CAD or STL data or data obtained using a different method of nondestructive testing can be used. In most cases, the a priori data available does not coincide with the measured CL data concerning orientation and scale of the test object and therefore cannot be used without prior registration. This implies the need for a preprocessing step

determining the transformation which positions the a priori data to properly fit the measured projections.

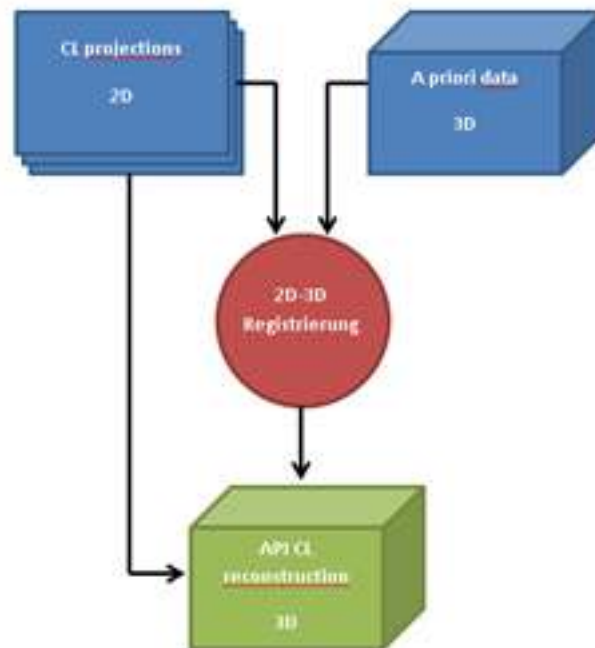


Figure 2. A priori reconstruction based on 2D-3D registration.

3. Registration Algorithm

The obvious approach of reconstructing the measured CL data to obtain a 3D volume which can be registered to the a priori data of the same dimensionality cannot be pursued as the traditional CL reconstruction will be degraded by blurring artefacts. Thus, instead of using a 3D-3D registration algorithm, the 2D projections are to be registered directly with the 3D a priori data, without prior reconstruction (Fig. 2). A new algorithm solving this 2D-3D registration problem was developed and is discussed in the following. In order to register a given a priori volume, an affine transformation that consists of rotation, translation and scaling is to be applied to the laminographic data. The components rotation and translation will be discussed in the following; solely the computation of the scale factor is not described as the scaling problem can be solved by suitable preprocessing of the a priori volume.



Figure 3. Reference CLARA Projections for rotation angles 0°, 120° and 240°.

Although a set of measured CL data usually consists of more than a hundred projections, each corresponding to a different rotation angle of the object, only three of these projections are

used in the following computations. In theory, the information contained in three transmission images taken from different directions is sufficient for a unique determination of all the unknowns in such an affine transformation. For greater stability and reliability of the algorithm, the angular difference of these three reference projections should be maximal, i.e. approximately 120° , as shown in an example of a circuit board in figure 3. The a priori volume of this circuit board is pictured in figure 4.

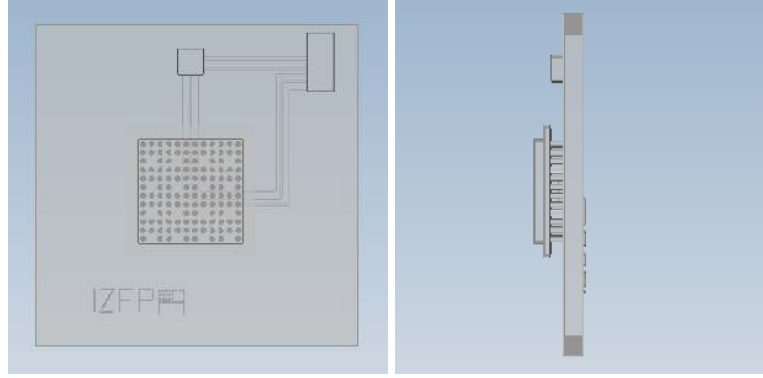


Figure 4. A priori volume, frontal and lateral view (transparent).

3.1 Rotation

In order to obtain the rotation, the search space of all 3-d rotations in space is sampled equidistantly and the sampled rotations are evaluated as will be explained in the following. Each element of the search space D_R consists of two angles $\theta, \varphi \in [0, \pi)$ which correspond to the spherical coordinates of the unit rotation axis and another angle $\alpha \in [0, 2\pi)$ giving the rotation angle. To find an equidistant sampling of the rotation axes, θ and φ need to be sampled non-equidistantly as the transformation from spherical coordinates to world coordinates is non-linear. Once a sampling of the search space is found, each rotation to be evaluated is applied to the geometry of the given CL data (which consists of three projections and the corresponding geometry settings). The modified geometry data is used in the simulation of projections of the a priori volume. Regarding the object orientation, these projections are to be compared to the original CL projections in order to find an evaluation of the rotation applied. In case the object orientation is identical in all three projection pairs, the rotation applied is the unique rotation allowing for the registration of the object's orientation in a priori and CL data. Finding a reasonable evaluation value is challenging since the grey values of the projection pairs cannot be compared directly because of the different image acquisition methods. Comparability can be achieved by binarization (or trinarization) of the projection, i.e. segmentation in 2 or 3 different areas. In order to segment the projection into two areas, distinguishing between pixels that were hit by X-rays either having passed any material on their way from source to detector or not, a single threshold is used. This threshold is found in a way similar to Otsu's method [6]. Otsu starts with computing the variances of the two classes the image is divided into by a threshold $T \in \mathbb{N}$. The 'ideal' threshold is selected as the one minimizing the intra-class variances, or, completely equivalent, maximizing the between-class variance. Let $\omega(T)$ be the probability of the 'material class' (consisting of all pixels with grey value $< T$), $\mu_0(T)$ and $\mu_1(T)$ the means of the material and the 'air class' and μ the whole projections' mean. The between class variance, which is minimized in Otsu's method, is given by

$$\sigma^2(T) = \omega(t)(\mu_0(T) - \mu)^2 + (1 - \omega(t))(\mu_1(T) - \mu)^2 \quad (3)$$

with $c = 2$. In the algorithm introduced here, the parameter c is chosen greater than 2 resulting in a higher weight on a small intra-class variance of the air class than one on a small intra-class variance of the material class. This is reasonable as the air class is to consist only of pixels that were hit by x-rays not having crossed any material and therefore having been hardly attenuated on their path. Thus the variance of grey-values within this class should be very small, whereas the variance within the material class may be significantly higher. In some cases, distinguishing a third projection segment allowing for more distinguishable evaluations can be necessary. Therefore, a third class of pixels, containing those that were hit by very strongly attenuated x-rays and therefore corresponding to denser material, is defined. To accomplish such a distinction, another binarization using a single threshold is performed on the material class. In this case, the threshold is found by computing a specified quantile of the material class's pixel values. As the translation is not known yet, the objects can be positioned differently within the projection pairs. To compensate for this, object barycenters are computed by averaging over all border pixels of the material class and these barycenters are moved to the projection center. Once the preprocessing is completed, the rotation's evaluation value can be computed as

$$\Delta(d) = \frac{1}{3} \sum_{i=1}^3 \frac{1000}{n^2} \sum_{j=1}^n \sum_{k=1}^n \left((p_i^R)_{(j,k)} - (p_i^E(d))_{(j,k)} \right)^2 \quad (4)$$

where p^R are the centered CL projections and $p^E(d)$ the centered simulated projections for rotation $d \in D_R$. To find the ideal rotation, an iterative approach is used. After having evaluated all rotations of the first rotation set, the best or a number of best rotations are selected, in doing so only local minima on the initial set may be picked. Around each such rotation, a refined equidistant grid of rotations that are to be evaluated in the following iteration is computed. This procedure is repeated until the grid distance falls below a certain threshold and thus, the local minima are approximated sufficiently exactly. As the evaluation mapping $\Delta: D_R \rightarrow \mathbb{R}$ is not convex and may have a large number of local minima, such an iterative procedure tracking different local minima is necessary in order to find the global minimum. Still, this is only possible if grid distance in the initial set of rotations is sufficiently small. In some cases, especially in case of binary a priori data, an initial rotation allowing for convergence against the unique global minimum may be inevitable.

3.2 Translation

The three-dimensional translation vector is computed after scaling and rotation have already been found, thus one can assume three pairs of projections showing the object in identical orientations. For each projection an image barycenter is computed and, by subtraction, a two-dimensional translation is found for each pair of projections as illustrated in figure 5.

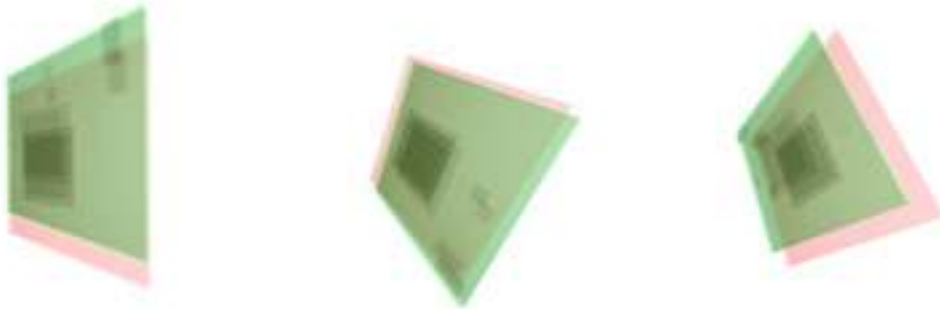


Figure 5. Pairs of projections, red measured CL data, green simulated projections.

One can compute corresponding 3D translations within the detector plane as the detector orientation for each rotation angle is known from the CL measurement's geometry data. These translations are projections of the actual object translation $x \in \mathbb{R}^3$ onto the detector plane in respective X-ray directions. Thus, it holds

$$x = \frac{1}{f} \cdot t_i + \lambda_i \cdot s_i \quad (5)$$

with $f \in \mathbb{R}$ the geometry-dependent magnification factor, $t_i \in \mathbb{R}^3$ the translation vectors computed from projection pairs and geometry, $q_i \in \mathbb{R}^3$ the x-ray transmission direction to the simulated projection's barycenter and real numbers $\lambda_i \in \mathbb{R}$, $i = 1, 2, 3$. Due to small variations in the object's actual magnification depending on its exact position, this formula is not completely accurate. The translation x can be found by solving

$$\operatorname{argmin}_x \min_{\lambda \in \mathbb{R}^3} \left(\sum_{i=1}^3 \left\| \left(\frac{1}{f} \cdot t_i + \lambda_i \cdot s_i \right) - x \right\|^2 \right) \quad (6)$$

Computation of this convex function's gradient and setting it equal to zero yields a linear system of six equations. The translation allowing for registration of a priori and CL data is then obtained by solving this linear system of equations.

4. Experiments

To justify the algorithm, simulated data of a circuit board with a fracture is used. The projections were simulated using CLARA geometry; a voxel volume containing a defect free version of the circuit board was computed by the simulation software Scorpius XLab and is used as a priori model. The a priori volume was consecutively rotated by -26° around the x-axis, 40° around the y-axis and 72° around the z-axis which is equivalent to a single rotation of 76.38° around the axis $(-0.5934, 0.2351, 0.7698)$. An additional translation by the vector $(-1.0, -1.4, -0.8)$ was applied. This information is used to easily determine the algorithm's accuracy.

Table 1 summarizes the parameters of translation and rotation which were computed using the 2D-3D registration algorithm and compares these values to the actual transformation applied to the a priori volume. The computed rotation angles deviate by less than 0.0015% from the ground truth. For the translation vector, the maximal deviation is 3.4 % for the z-component, and clearly less for the other two components (0.81% and 0.58%). The accuracy depends on the bi- and trinarization thresholds which are applied to the projection sets to be compared. At the same time, precision can be increased by using larger projections due to the greater number of pixels contained.

Table 1. Difference between computed and actual transformation parameters

Axis	Translation computed [cm]	Translation [cm]	Rotation computed [°]	Rotation [°]
x	-1.0081	-1.0	-26.0038	-26.0
y	-1.4081	-1.4	40.0005	40.0
z	-0.8275	-0.8	71.9911	72.0

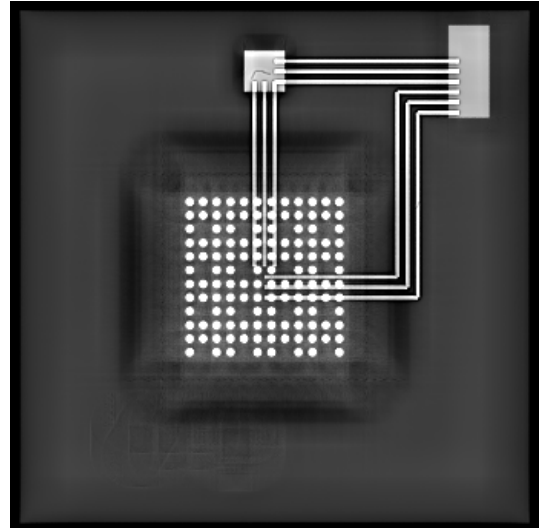
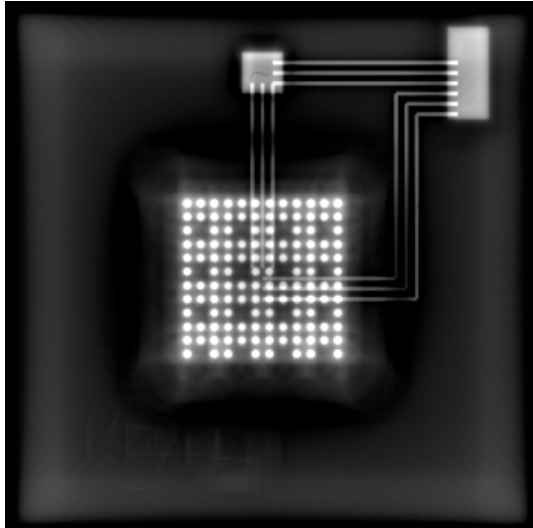


Figure 6. Circuit board phantom, frontal view, left SART, right AP-SART using registered a priori volume.

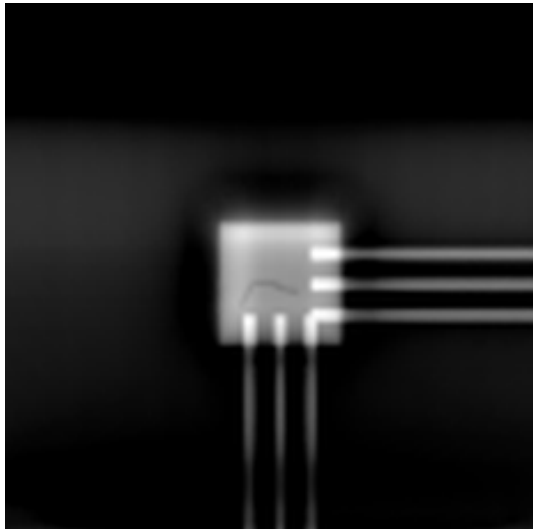


Figure 7. Circuit board phantom, frontal view, magnified, left SART, right AP-SART using registered a priori volume.

The gain in quality that can be achieved by the use of registered a priori information is illustrated in a few figures: In the reconstruction's frontal views shown in figure 6 and 7 the defect, a branched crack, is clearly better visible when registered a priori information is used. Figure 8 and 9 show the lateral views of the reconstructed volumes. The images demonstrate that the blurring artefacts can be drastically reduced by the use of a priori information. While the circuit board's contours cannot be recognized in the traditional reconstruction, the a priori reconstruction not only shows the edges sharply but also allows the defects to be detected. In this lateral view the crack within the circuit board's base card consists of two branches and thus is visible as two porosities in the magnified AP SART reconstruction, which cannot be discerned in the normal SART reconstruction without a priori information.



Figure 8. Circuit board phantom, lateral view, left SART, right AP-SART using registered a priori volume.

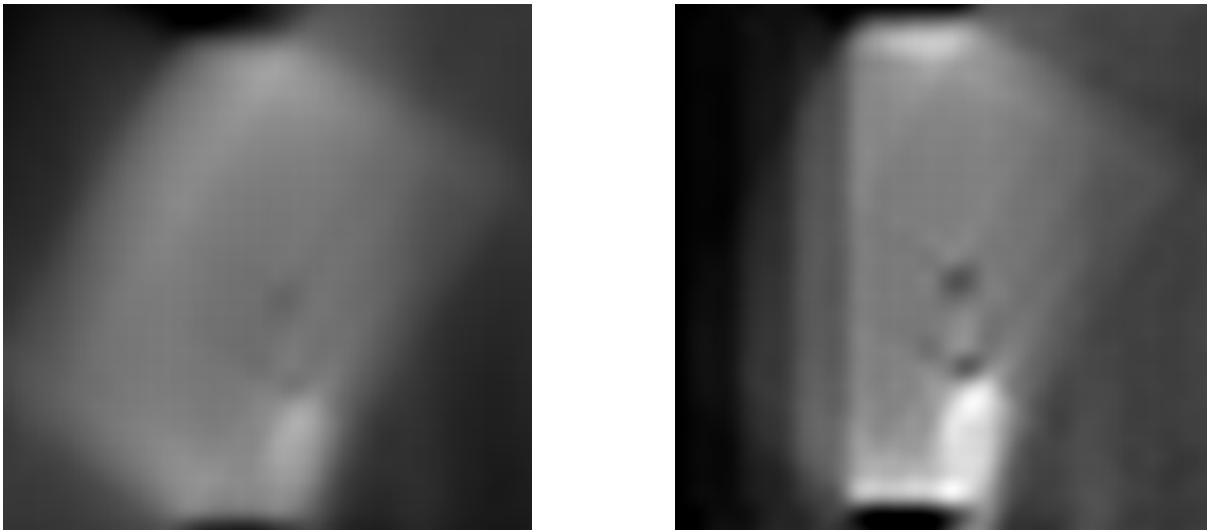


Figure 9. Circuit board phantom, lateral view, magnified defect area, left SART, right AP-SART using registered a priori volume.

4. Conclusion

The use of a priori information in the reconstruction of laminographic measurement data can dramatically increase the quality of the resulting volume and thus enables the detection of defects which cannot be identified within the traditionally reconstructed volume. The algorithm presented in this work successfully registers 2D CL data with 3D a priori models and therefore allows for an effective use of given a priori knowledge in the SART reconstruction process. Apart from its benefits for computed laminography this technique is also very useful for classic CT, for instance reducing the number of projections needed for sufficient reconstruction quality and thereby minimizing the measurement and reconstruction time.

The work was partially funded by the DFG in the project "Parallel Iterative Methods with A Priori Information for Robust Computed Laminography of Low Contrast, Difficult-To-Measure Objects".

References

1. Maisl, M.; Porsch, F.; Schorr, C., Computed Laminography for X-ray Inspection of Lightweight Constructions, International Symposium on NDT in Aerospace. Berlin : Deutsche Gesellschaft für zerstörungsfreie Prüfung (DGZfP), 2010 (DGZfP-Berichtsbände 124)
2. Andersen, A.; Kak, A., Simultaneous algebraic reconstruction technique (SART): a superior implementation of the art algorithm. Ultrason Imaging, 6(1):81–94, 1984
3. Schorr, C.; Maisl, M., Exploitation of geometric a priori knowledge for limited data reconstruction in non-destructive testing, Proceedings of the Fully3D Conference 2013, pp 114-117, 2013.
4. Schorr, C., Maisl, M., A ray-length-based ROI-correction for computed laminography, Proceedings of 5th Conference on Industrial Computed Tomography 2014, pp. 253-258, 2014, ISBN: 978-3-8440-2557-6.
5. M. Franz. EAR - Einsatzsynchrone Artefakt Reduktion, PhD thesis, Friedrich-Alexander-Universität Erlangen-Nürnberg, 2009.
6. Nobuyuki Otsu. A threshold selection method from gray-level histograms. Automatica, 11(285-296):23-27, 1975.
7. Dörr, L. Registrierung von a priori Volumina in der Computerlaminographie, Masterthesis, Universität des Saarlandes, Saarbrücken, 2015.